

Oxidative *ortho*-C-N Fusion of Aniline by OsO₄. Isolation, Characterization of Oxo-Amido Osmium(VI) Complexes, and their Catalytic Activities for Oxidative C–C Bond Cleavage of Unsaturated Hydrocarbons

Subhas Samanta,[†] Laksmikanta Adak,[‡] Ranjan Jana,[‡] Golam Mostafa,[§] Heikki M. Tuononen,^{||} Brindaban C. Ranu,[‡] and Sreebrata Goswami^{*†}

Department of Inorganic Chemistry and Department of Organic Chemistry, Indian Association for the Cultivation of Science, Kolkata 700 032, India, Department of Physics, Jadavpur University, Kolkata 700 032, India, and Department of Chemistry, University of Jyväskylä, P.O. Box 35, Jyväskylä FI-40014, Finland

Received July 19, 2008

In an unusual reaction of osmium(VIII) oxide with *p*-substituted aromatic amines (X-C₆H₄-NH₂, where X = Me, H, Cl) in heptane afforded the brown osmium(VI)-oxo complexes [OsO(L)₂] (**1a-c**, L = N-aryl-1,2-arylenediamide) in moderate yields. The ligand L is formed *in situ* via oxidative *ortho*-C-N fusion of arylamines. The reaction occurs in an inert atmosphere, and a part of Os(VIII) is used up for the oxidation of aromatic amine. Single crystal X-ray structure of a representative complex **1a** is solved. The structural analysis has authenticated the *ortho*-C-N fusion of ArNH₂ resulting in formation of the diamide ligand, L. The complex as a whole is penta-coordinated, and the coordination sphere has a distorted square pyramidal geometry ($\tau = 0.26$). A similar reaction of osmium(VIII) oxide with the preformed N-phenyl-1,2-phenylene diamine produced the complex **1a** in nearly quantitative yield. The substituted phenazine, 5-phenyl-3-phenylimino-3,5-dihydro-phenazine-2-ylamine, is obtained as a byproduct of the latter reaction. The complexes, **1a-c**, can be reduced in a reversible one-electron step, as probed by cyclic voltammetry. The one electron reduced paramagnetic Os(V) intermediate is, however, Electron Paramagnetic Resonance (EPR) silent. Solution spectra of the osmium complexes show several multiple transitions in the UV–vis region. Density functional theory calculations were employed to confirm the structural features and to support the spectroscopic assignments. The complex **1a** catalyzes oxidation of a wide variety of unsaturated hydrocarbons like alkenes, alkynes, and aldehydes to the corresponding carboxylic acids in the presence of *tert*-butylhydroperoxide (TBHP) efficiently at room temperature.

Introduction

Organo-imido complexes including those of osmium(VIII) have been one of the most researched kinds of compounds primarily because these are potential intermediates^{1–7} for organic reactions involving the formation of nitrogen–carbon

bonds. However, to date only a limited number of stable osmium(VIII) imido species have actually been isolated.⁸ Monoimido osmium(VIII) complexes are accessible directly from OsO₄ with the tertiary alkyl amines in hydrocarbon

* To whom correspondence should be addressed. E-mail: icsg@iacs.res.in.

[†] Department of Inorganic Chemistry, Indian Association for the Cultivation of Science.

[‡] Department of Organic Chemistry, Indian Association for the Cultivation of Science.

[§] Jadavpur University.

^{||} University of Jyväskylä.

(1) (a) Nugent, W. A.; Mayer, J. M. *Metal Ligand Multiple Bonds*; Wiley: New York, 1988. (b) Wigley, D. E. *Prog. Inorg. Chem.* **1994**, *42*, 239.

(2) (a) Berrisford, D. J.; Bolm, C.; Sharpless, K. B. *Angew. Chem.* **1995**, *107*, 1159; *Angew. Chem., Int. Ed.* **1995**, *34*, 1059. (b) Bruncko, M.; Khuong, T.-A. V.; Sharpless, K. B. *Angew. Chem., Int. Ed. Engl.* **1996**, *35*, 454.

(3) Sharpless, K. B.; Hori, T.; Truesdale, L. K.; Dietrich, C. O. *J. Am. Chem. Soc.* **1976**, *98*, 276.

(4) Chong, A. O.; Oshima, K.; Sharpless, K. B. *J. Am. Chem. Soc.* **1977**, *99*, 3420.

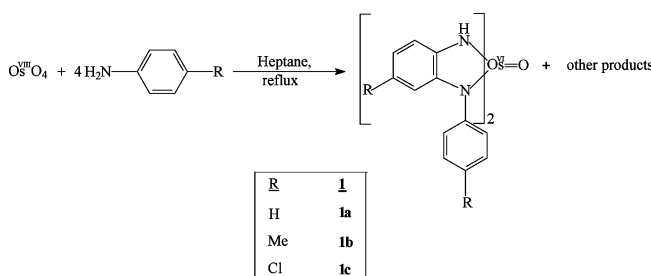
(5) (a) Muñiz, K.; Nieger, M. *Synlett.* **2003**, 211. (b) Muñiz, K.; Iesato, A.; Nieger, M. *Chem.—Eur. J.* **2003**, *9*, 5581. (c) Muñiz, K.; Nieger, M.; Mansikkamäki, H. *Angew. Chem.* **2003**, *115*, 6141; *Angew. Chem., Int. Ed.* **2003**, *42*, 5958. (d) Muñiz, K. *Eur. J. Org. Chem.* **2004**, 2243.

(6) Donohoe, T. J. *Synlett* **2002**, 1223.

solvent or even with aqueous amine solution.^{8–10} In contrast the corresponding reactions with aromatic amines have been confined¹¹ only to 2,6-disubstituted bulky arylamines. It has been reported that the similar reaction of unsubstituted aniline with OsO₄ leads to degradation¹² together with the formation of unidentified azo compounds. In this paper we disclose the synthesis of a family of square pyramidal mono-oxo diamido osmium(VI) complexes from an unprecedented reaction of OsO₄ and aniline, or its substituted derivatives. In this reaction the *ortho*-unsubstituted anilines undergo oxidative C–N bond fusion to produce doubly deprotonated N-aryl-1,2-phenylenediamides. Our interest in these reactions originated from our previous results¹³ on transition metal mediated oxidative *ortho*-C-N fusion of aromatic amines. The reactions occur because of *ortho*-C-H activation as a consequence of metal coordination. Furthermore, we have shown before^{13a,14,15} that the *cis*-coordination of the aromatic amines is a prerequisite for the above *ortho*-fusion reaction. Our work in this area has so far been confined to the use of Ru(III) and Os(IV) nonoxo compounds as mediators. In this work OsO₄ was chosen as a mediator since first, it is an exceptionally strong oxidant, and second, its lability toward substitution by amines is documented⁸ in the literature. These two properties are in fact essential for the above aromatic amine fusion reactions. The reactions have produced penta-coordinated mono-oxo osmium(VI) complexes of N-aryldiamides as the only major product.

Interestingly the above osmium(VI) oxo complexes are found to catalyze oxidative cleavage of C–C bonds in unsaturated hydrocarbons like alkenes and alkynes by *t*-butylhydroperoxide at room temperature. Notably, since 1980s there have been exciting developments in the high valent ruthenium-oxo complexes, some of which are useful and active oxidants^{16,17} for organic substrates. In comparison,

Scheme 1



osmium-oxo complexes are much weaker oxidants^{17d} than the corresponding ruthenium complexes and a suitable osmium complex catalyst^{18–20} for oxidative cleavage of unsaturated hydrocarbons is scarce in the literature.

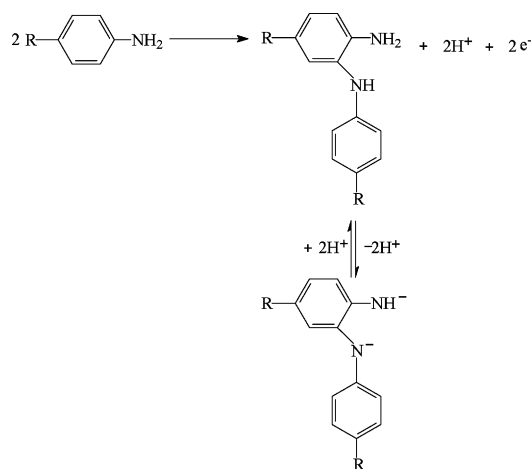
Results and Discussion

Synthetic Reaction. Since we are interested in dimerization and/or polymerization of aromatic amines by *ortho*-C-N bond fusion, we purposefully chose aromatic amines without any *ortho*-substitution (like aniline and its *para*-substituted derivatives) for the reaction. The reactions of OsO₄ with primary aromatic amines proceeded smoothly in heptane producing penta-coordinated oxo-amido osmium (VI) complexes **1a–c** as shown in Scheme 1. Isolated yields of the products after TLC purification were nearly 40%; a mixture of unidentified brown products also formed along with **1**. We wish to note here that a similar reaction with 2,6-dichloroaniline failed to produce any identifiable product. The organic reaction, as shown in Scheme 2, involves 2e[−] oxidation of aromatic amines. Thus, the formation of the bis-chelate, **1** (Scheme 1) from 4ArNH₂ and OsO₄ needs a transfer of a total of four electrons. In comparison, the metal oxidation level in the product **1** is only two units less than that in the starting compound OsO₄. The fact that the reference reaction also proceeded smoothly in an inert atmosphere producing **1** in a similar yield excluded the possibility of involvement of aerial oxygen in this oxidation reaction. Thus, it is anticipated that half of OsO₄ is expended as oxidant²¹ which, in turn, justifies the moderate yields of **1** (<50%) from the above reactions. For further elucidation of the above electron accounting issue, a reaction of OsO₄ and the preformed ligand, N-phenyl-1,2-phenylenediamine

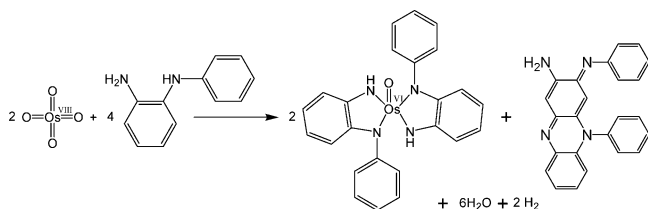
- (7) Donohoe, T. J.; Blades, K.; Moore, P. R.; Waring, M. J.; Winter, J. J. G.; Helliwell, M.; Newcombe, N. J.; Stemp, G. *J. Org. Chem.* **2002**, *67*, 7946.
- (8) Muñiz, K. *Chem. Soc. Rev.* **2004**, *33*, 166.
- (9) (a) Milas, N. A.; Iliopoulos, M. I. *J. Am. Chem. Soc.* **1959**, *81*, 6089. (b) Clifford, A. F.; Kobayashi, C. S. *Inorg. Synth.* **1960**, *6*, 207.
- (10) Sharpless, K. B.; Patrick, D. W.; Truesdale, L. K.; Biller, S. A. *J. Am. Chem. Soc.* **1975**, *97*, 2305.
- (11) (a) Anhaus, J. T.; Kee, T. P.; Schofield, M. H.; Schrock, R. R. *J. Am. Chem. Soc.* **1990**, *112*, 1642. (b) Schofield, M. H.; Kee, T. P.; Anhaus, J. T.; Schrock, R. R.; Johnson, K. H.; Davis, W. M. *Inorg. Chem.* **1991**, *30*, 3595.
- (12) Danopoulos, A. A.; Wilkinson, G.; Hussain-Bates, H.; Hursthouse, M. B. *J. Chem. Soc., Dalton Trans.* **1991**, 269.
- (13) (a) Mitra, K. N.; Goswami, S. *Inorg. Chem.* **1997**, *36*, 1322. (b) Mitra, K. N.; Majumdar, P.; Peng, S.-M.; Castiñeiras, A.; Goswami, S. *Chem. Commun.* **1997**, 1267. (c) Mitra, K. N.; Choudhury, S.; Castiñeiras, A.; Goswami, S. *J. Chem. Soc., Dalton Trans.* **1998**, 2901. (d) Mitra, K. N.; Goswami, S. *Chem. Commun.* **1997**, 49. (e) Das, C.; Goswami, S. *Comments Inorg. Chem.* **2003**, *24*, 137. (f) Majumdar, P.; Falvello, L. R.; Tomás, M.; Goswami, S. *Chem.—Eur. J.* **2001**, *7*, 5222.
- (14) Mitra, K. N.; Peng, S.-M.; Goswami, S. *Chem. Commun.* **1998**, 1685.
- (15) Das, C.; Saha, A.; Hung, C.-H.; Peng, S.-M.; Goswami, S. *Inorg. Chem.* **2003**, *42*, 198.
- (16) RuO complexes: (a) Stultz, L. K.; Binstead, R. A.; Reynolds, N. S.; Meyer, T. J. *J. Am. Chem. Soc.* **1995**, *117*, 2520. (b) Ho, C.; Che, C.-M.; Lau, T.-C. *J. Chem. Soc., Dalton Trans.* **1990**, 967. (c) Fung, W. H.; Yu, W. Y.; Che, C.-M. *J. Org. Chem.* **1998**, *63*, 7715. (d) Bryant, J. R.; Mayer, J. M. *J. Am. Chem. Soc.* **2003**, *125*, 10351. (e) Lebeau, E. L.; Binstead, R. A.; Meyer, T. J. *J. Am. Chem. Soc.* **2001**, *123*, 10535. (f) Che, C.-M.; Yip, W.-P.; Yu, W.-Y. *Chem. Asian J.* **2006**, *1*, 453.

- (17) RuO₂ complexes: (a) Bailey, C. L.; Drago, R. S. *Chem. Commun.* **1987**, 179. (b) Goldstein, A. S.; Beer, R. H.; Drago, R. S. *J. Am. Chem. Soc.* **1994**, *116*, 2424. (c) Goldstein, A. S.; Drago, R. S. *J. Chem. Soc., Chem. Commun.* **1991**, 21. (d) Yip, W.-P.; Yu, W.-Y.; Zhu, N.; Che, C.-M. *J. Am. Chem. Soc.* **2005**, *127*, 14239. (e) Che, C.-M.; Yu, W.-Y.; Chang, P.-M.; Cheng, W. C.; Peng, S.-M.; Lau, K.-C.; Li, W.-K. *J. Am. Chem. Soc.* **2000**, *122*, 11380. (f) Cheng, W.-C.; Yu, W.-Y.; Li, C.-K.; Che, C.-M. *J. Org. Chem.* **1995**, *60*, 6840. (g) Cheng, W.-C.; Yu, W.-Y.; Cheung, K.-K.; Che, C.-M. *J. Chem. Soc., Chem. Commun.* **1994**, 1063.
- (18) Che, C.-M.; Cheng, W.-K.; Mak, T. C. W. *J. Chem. Soc., Chem. Commun.* **1986**, 200.
- (19) (a) El-Hendawy, A. M.; Griffith, W. P. *J. Chem. Soc., Dalton Trans.* **1989**, 901. (b) Griffith, W. P.; Jolliffe, J. M. *J. Chem. Soc., Dalton Trans.* **1992**, 3483. (c) Bailey, A. J.; Griffith, W. P.; Savage, P. D. *J. Chem. Soc., Dalton Trans.* **1995**, 3537.
- (20) Valliant-Saunders, K.; Gunn, E.; Shelton, G. R.; Hrovat, D. A.; Borden, W. T.; Mayer, J. M. *Inorg. Chem.* **2007**, *46*, 5212.
- (21) Soper, J. D.; Kaminsky, W.; Mayer, J. M. *J. Am. Chem. Soc.* **2001**, *123*, 5594.

Scheme 2



Scheme 3



(*o*-semidine) was performed under identical reaction conditions. In this case the isolated yield of **1a** was 94%. However, a higher ligand stoichiometry (OsO_4 : *o*-semidine = 1:3) was necessary for completion of the reaction. The excess ligand used herein brings about the metal reduction $\text{Os(VIII)} \rightarrow \text{Os(VI)}$ at the cost of its self-oxidation^{22,23} to 5-phenyl-3-phenylimino-3,5-dihydro-phenazine-2-ylamine (Scheme 3). The substituted phenazine compound was isolated from the reaction mixture and characterized. A similar reaction of OsO_4 with 1,2-diaminobenzene was reported²⁴ to give $[\text{Os}^{\text{VII}}\text{O}_2(\text{opda})_2]$ (*opda* = 1,2-diaminobenzene).

It is believed that the reference reaction occurs because of induced *ortho*-C-H activation of a coordinated aryl amido intermediate. However, there may be several possibilities which remain unresolved because of the lack of chemical information of the intermediates. We wish to note here that such OsO_4 mediated dimerization of aromatic amines is unknown in the literature. Mayer and co-workers, recently, have reported^{21,25} a few examples of nucleophilic aromatic substitution at the *para* carbon of a coordinated anilido ligand in a substitutionally inert Os(IV) complex. We thus conclude that *cis*-disposition of the coordinated aryl-amido ligands in the intermediate complex is possibly the key for the *ortho*-C-N fusion reactions.

The osmium complexes **1a-c** analyzed satisfactorily; their electrospray ionization mass spectrometry (ESI-MS) spectra

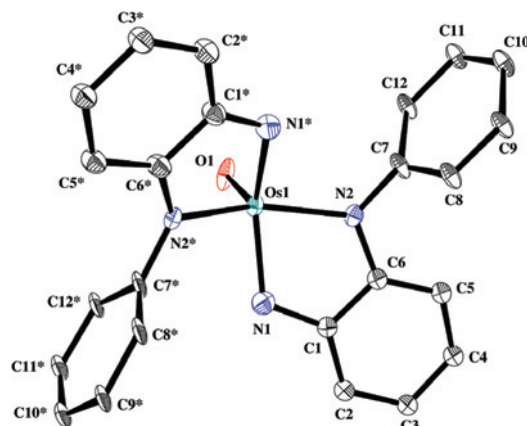


Figure 1. ORTEP representation and atom numbering scheme for $[\text{OsO}(\text{L}^{\text{a}})_2]$ (**1a**).

exactly corroborated with their simulated spectra. Appearance of strong bands near 3400 and 890 cm^{-1} in the IR-spectra characterize the presence of N–H and $\text{Os}=\text{O}$ fragments, respectively. The NMR spectra (^1H as well as ^{13}C) of the representative complexes are submitted as Supporting Information, Figure S1 and S2). Notably, the two ligands in the complexes are magnetically equivalent because of the presence of a 2-fold rotational symmetry axis (see below), and hence, resonances for only one ligand were observed. For example, the complex **1b** showed only two methyl proton resonances at δ 2.55 and 2.30 ppm, respectively. The amide N–H proton of **1a** appeared at δ 4.5 ppm, which exchanges with D_2O resulting in disappearance of the resonance. ^{13}C NMR and DEPT spectra of the complexes are found to be informative for their characterization. For instance, the reactant Ph-NH_2 has only one quaternary carbon, while the DEPT spectrum of the compound **1a** indicated the presence of three such carbon atoms confirming the formation of *o*-semidine from aniline via C–N fusion. Similarly, five quaternary carbon atoms in the 4-substituted compounds **1b** and **1c** were observed as expected.

Crystal Structure. Final characterization of the complexes came from the analysis of the X-ray structure of the representative complex **1a**. Suitable crystals for X-ray structure determination were obtained by slow diffusion of a dichloromethane solution of the compound **1a** into hexane. The structure analysis of **1a** indeed confirmed the regioselective *ortho*-fusion of ArNH_2 . Its Oak Ridge Thermal Ellipsoid Plot (ORTEP) and atom numbering scheme are depicted in Figure 1. The molecule **1a** is penta-coordinated and the coordination sphere has a distorted square pyramidal geometry ($\tau = 0.26$). It is a bis-chelated Os(VI) complex of N-phenyl-1,2-phenylene diamide ligand in which the oxide ligand (O1) occupies the fifth position. A 2-fold rotational axis of symmetry passes through the $\text{Os}=\text{O}$ bond with the four basal nitrogen atoms (N1,N2,N1*, N2*); * = $1/2 - x, y, 1/2 - z$) in an essentially planar orientation. The osmium atom lies above the plane by 0.580 \AA toward the oxide ligand. The Os-N bond lengths are in the range $1.965(21)$ – $1.981(10) \text{ \AA}$ and the Os-O1

(22) Chlopek, K.; Bill, E.; Weyhermüller, T.; Wieghardt, K. *Inorg. Chem.* **2005**, *44*, 7087.

(23) Ghosh, A. K.; Mitra, K. N.; Mostafa, G.; Goswami, S. *Eur. J. Inorg. Chem.* **2000**, 1961.

(24) Danopoulos, A. A.; Wong, A. C. C.; Wilkinson, G.; Hursthouse, M. B.; Hussain, B. *J. Chem. Soc., Dalton Trans.* **1990**, 315.

(25) Soper, J. D.; Saganic, E.; Weinberg, D.; Hrovat, D. A.; Benedict, J. B.; Kaminsky, W.; Mayer, J. M. *Inorg. Chem.* **2004**, *43*, 5804.

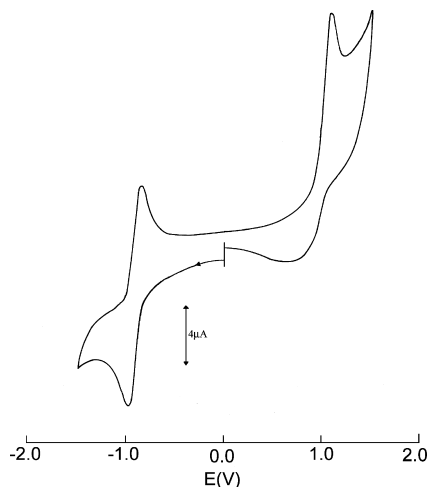


Figure 2. Cyclic voltammogram of **1a** in CH₂Cl₂/0.1 M Bu₄NClO₄.

Table 1. Selected Experimental and Calculated Bond Lengths (Å) and Angles (deg) of **1a**

	1a	
	exp.	calc.
Os1–O1	1.676(13)	1.721
Os1–N1	1.965(21)	1.941
Os1–N2	1.981(10)	1.995
N1–C1	1.352(24)	1.376
N2–C6	1.307(17)	1.390
N2–C7	1.380(17)	1.409
C1–C2	1.396	1.390
C2–C3	1.387	1.387
C3–C4	1.389	1.392
C4–C5	1.389	1.387
C5–C6	1.390	1.393
O1–Os1–N1	107.1(6)	114.8
O1–Os1–N2	107.2(3)	103.8
N1–Os1–N2	77.8(7)	78.5

bond length is 1.676(13) Å, (see Table 1) indicating its double bond²⁶ character.

Cyclic Voltammetry. The redox behavior of the diamido complexes **1a–c** was studied by cyclic voltammetry in dichloromethane (0.1 M TBAP) in the potential range between +1.5 and –1.5 V and using a platinum working electrode. The potentials are referenced to the saturated Ag/AgCl electrode. The cyclic voltammogram of **1a** is displayed in Figure 2 as an illustrative example. It shows two one-electron redox processes in the above potential range. A reversible reductive response appeared near –1.0V; the second response is irreversible and occurs at an anodic potential, about +1.0V. The reversible response at the cathodic potential corresponds to the reduction of the metal center while the process occurring at the positive potential formally corresponds to the ligand oxidation. The potentials of the above couples all vary linearly (Supporting Information, Figure S3) with respect to the Hammett $\Sigma\sigma_p$ parameter of the substitutions on the ligand. There is quite a large change in the donor character of the ligand over the above series of substituents (see Table 2).

One-electron stoichiometry of the reversible process was confirmed by exhaustive electrolysis of the representative

Table 2. Cyclic Voltammetry Data of **1a–c**^a

compound	oxidation $E_{1/2}$, ^b V	reduction $E_{1/2}$, ^b V (ΔE_p , mV)
1a	0.95 ^c	–0.97(75)
1b	1.01 ^c	–1.08(70)
1c	0.89 ^c	–0.79(75)

^a In dichloromethane solution, supporting electrolyte Bu₄NClO₄ (0.1 M).
^b $E_{1/2} = 0.5(E_{pa} + E_{pc})$ where E_{pa} and E_{pc} are anodic and cathodic peak potentials respectively. $\Delta E_p = E_{pa} - E_{pc}$, scan rate 50 mVs^{–1}. ^c Irreversible.

Table 3. Absorption Maxima of **1a–c** from UV-vis Spectra^a

complex	λ_{max}/nm ($\epsilon/M^{-1} cm^{-1}$)
1a	675 ^b , 535(6840), 430 ^b , 350(17285), 295 ^b , 260 ^b , 225(32810)
1b	690 ^b , 555(6245), 445 ^b , 355(17655), 300 ^b , 260 ^b , 230(29955)
1c	680 ^b , 540(5695), 545 ^b , 355(17195), 305 ^b , 260 ^b , 230(29240)

^a In CH₂Cl₂. ^b Shoulder.

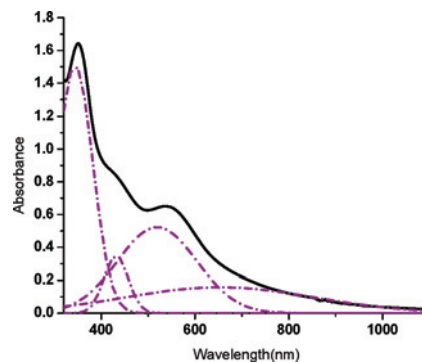


Figure 3. UV-vis spectrum of **1a** in CH₂Cl₂.

compound **1a** at –1.2 V. The electrogenerated one electron reduced species [**1a**][–] was, however, EPR silent. This is possibly due to high spin orbit coupling constant of Os(V), $\xi(\text{Os}^{5+})$ about 4500 cm^{–1}. Examples of EPR silent osmium(V) complexes²⁷ are known in the literature. These results are fully corroborated by density functional theory (DFT) calculations which show that the lowest unoccupied molecular orbital (LUMO) and highest occupied molecular orbital (HOMO) of complex **1a** are primarily metal and ligand centered, respectively (see below). Thus, one electron reduction of **1a** is expected to create an anionic osmium(V) system with a geometry similar to one observed for the neutral species. DFT optimization carried out for [**1a**][–] revealed only slight elongation (0.04 Å) of the Os=O and Os–N metrical parameters upon electron attachment which is in good agreement with the reduction of Os from VI to V.

UV-vis Spectra and DFT. The compounds **1a–c** exhibit rather similar low-energy absorption spectra with a weaker band near 680 nm and another near 550 nm (Table 3). Gaussian analyses of the overlapping bands are shown in Figure 3. The assignment of these bands is guided by the results from DFT calculations. Before calculation of the excitation energies using the time-dependent DFT (TDDFT) formalism, the molecular structure of **1a** was fully optimized at the BPBE1PBE/TZVP level of theory. The calculated bond lengths and angles (see data given in Supporting Information, Table S1) can be compared to the crystallographically established metrical parameters (Table 1). Overall there is a very good agreement with the two sets of numbers as bond

(26) Che, C.-M.; Lam, M. H.-W.; Wang, R.-J.; Mak, T. C. W. *J. Chem. Soc., Chem. Commun.* **1990**, 820.

(27) Dengel, A. C.; Griffith, W. P. *Inorg. Chem.* **1991**, *30*, 869.

Table 4. Calculated Singlet Transition Energies (> 300 nm) of **1a**

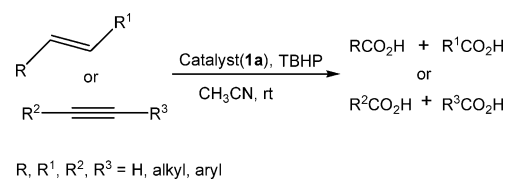
symmetry	energy [nm] ^a	dominant contributions (>5%)
a(1)	680 (0.0078)	HOMO → LUMO (92%)
a(2)	451 (0.0003)	HOMO → LUMO+1 (77%)
a(3)	387 (0.0038)	HOMO-3 → LUMO (17%) HOMO-1 → LUMO+1 (11%) HOMO-2 → LUMO+2 (8%)
a(4)	326 (0.0082)	HOMO-4 → LUMO (47%) HOMO-2 → LUMO+2 (44%)
a(5)	314 (0.0014)	HOMO-3 → LUMO+1 (83%) HOMO-4 → LUMO (10%)
b(1)	560 (0.0685)	HOMO-1 → LUMO (88%) HOMO-2 → LUMO (8%)
b(2)	436 (0.0619)	HOMO-2 → LUMO (86%) HOMO-1 → LUMO+1 (6%)
b(3)	399 (0.0588)	HOMO-1 → LUMO+1 (86%) HOMO → LUMO+2 (6%)
b(4)	370 (0.0048)	HOMO-8 → LUMO (68%) HOMO → LUMO+2 (19%) HOMO-5 → LUMO (8%)
b(5)	355 (0.1949)	HOMO → LUMO+2 (65%) HOMO-8 → LUMO (16%) HOMO-1 → LUMO+1 (6%) HOMO-2 → LUMO+1 (5%)
b(6)	321 (0.0528)	HOMO-2 → LUMO+1 (81%) HOMO-1 → LUMO+3 (7%) HOMO-2 → LUMO+2 (5%)

^a Oscillator strengths are reported in parenthesis.

lengths and angles are predicted within 2 pm and 1–4° from the experimental values, respectively. Interestingly, however, the four basal nitrogen atoms in the 1,2-diamido phenylene ligands are in a distinctly nonplanar orientation in the calculated structure though the X-ray analysis showed them to be in an essentially planar arrangement. This difference arises most likely from crystallographic packing of the coplanar N-phenyl groups as such interactions are not modeled in calculations.

The calculated excitation energies for **1a** are reported in Table 4. The low intensity tail observed in the experimental spectrum compares well with the calculated value for the HOMO → LUMO transition at around 680 nm. The two mid-intensity peaks with transition maxima close to 550 and 430 nm can be readily assigned to b(1) (HOMO-1 → LUMO) and b(2) (HOMO-2 → LUMO) transitions which are computationally predicted to appear at 560 and 436 nm, respectively. Several possible transitions were found to lie between 300–400 nm. However, calculated oscillator strengths predict that transitions b(3), b(5), and b(6) should dominate the spectrum. In fact, the highest oscillator strength is calculated for the b(5) transition (predominately HOMO → LUMO+2 in character) at 355 nm which is in excellent agreement with the experimentally observed band maximum close to 350 nm.

An analysis of the MOs of the complex **1a** reveals that the highest MOs are centered on the N-phenyl-1,2-phenylene ligands and are, thus, π -type in character (see Supporting Figure S4). The lowest unoccupied MOs have significantly smaller contributions from the two ligands and consist primarily of p and d orbitals on oxygen and osmium, respectively. Hence, the transitions given in Table 4 are all predominantly $\pi_L \rightarrow d_{Os} + p_O$ type.

Scheme 4

[1a]-Catalyzed Oxidation of Unsaturated Hydrocarbons. High valent metal-oxo complexes are attractive to chemists because of their abilities to catalyze the oxidation of alkenes by formal oxygen atom transfer reaction. Taking the advantages of the stability of high oxidation state of the present osmium complexes and their coordinative unsaturated nature, we set out to explore the possibilities of their application as catalysts. A representative complex, **1a** has been tested for this purpose. The reference complex indeed catalyzes oxidation of a wide variety of unsaturated hydrocarbons like alkenes, alkynes and aldehydes to the corresponding carboxylic acids in the presence of *tert*-butylhydroperoxide (TBHP) with remarkable efficiency at room temperature. We note here that usually the oxidative carbon–carbon bond cleavage reactions are achieved either by the cumbersome ozonolysis route²⁸ or by using^{29,30} RuO₄/NaOCl, RuO₄/IO₄⁻, and OsO₄/oxone reagents. Recently, Noyori et al. provided³¹ a green synthesis of adipic acid by the direct oxidation of cyclohexene using aqueous 30% H₂O₂ in the presence of a catalytic quantity of Na₂WO₄ and a phase transfer catalyst at 75–85 °C. Besides the above-noted metal oxides only selected examples of dioxo-ruthenium(VI) complexes are known to catalyze oxidative bond cleavage reactions.^{17d} The monooxo-ruthenium(IV) complexes, on the other hand, produce epoxides from olefins.¹⁶ Moreover, the examples of regioselective C–C bond cleavage of unsaturated hydrocarbons particularly those having less nucleophilic character, as in chalcones, are scarce.³²

Catalytic oxidation of a number of alkenes to carboxylic acids using non-aqueous *t*-BuOOH (TBHP) as the terminal oxidant and OsOL₂ (**1a**) as the catalyst proceeded cleanly under homogeneous condition at room temperature. Catalyst to substrate molar ratios of 0.5–1:100 and excess of TBHP over the stoichiometric quantity of the oxidant were employed. The reactions involve C–C bond breaking process (Scheme 4) yielding carboxylic acids. Pertinent results are summarized in Tables 5 and 6. Similar reaction using 70% aqueous TBHP produced the carboxylic acid as the major product; corresponding 1,2 diols, though in minor quantities

- (28) (a) Bailey, P. S. *Chem. Rev.* **1958**, *58*, 925. (b) Criegee, R. *Angew. Chem., Int. Ed. Engl.* **1975**, *14*, 745. (c) Larock, R. C. In *Comprehensive Organic Transformations*, 2nd ed.; Wiley-VCH: New York, 1999; pp 1213–1215. (d) Ogle, R. A.; Schumacher, J. L. *Process. Saf. Prog.* **1998**, *17*, 127. (e) Koike, K.; Inou, G.; Fukuda, T. *J. Chem. Eng. Jpn.* **1999**, *32*, 295.
- (29) (a) Sica, D. *Recent Res. Dev. Org. Chem.* **2003**, *7*, 105. (b) Courtney, J. L. *Organic Synthesis and Oxidation with Metal Compounds*; Mijs, W. J., Cornelis, R. H. I., Eds.; Plenum: New York, 1986; p 445.
- (30) (a) Travis, B. R.; Narayan, R. S.; Borhan, B. *J. Am. Chem. Soc.* **2002**, *124*, 3824. (b) Whitehead, D. C.; Travis, B. R.; Borham, B. *Tetrahedron Lett.* **2006**, *47*, 3797.
- (31) (a) Noyori, R.; Aoki, M.; Sato, K. *Chem. Commun.* **2003**, 1977. (b) Sato, K.; Aoki, M.; Noyori, R. *Science* **1998**, *281*, 1646.
- (32) (a) Kogan, V.; Quintal, M. M.; Neumann, R. *Org. Lett.* **2005**, *7*, 5039.

Table 5. Oxidation of Alkenes by TBHP Catalyzed by 1a

Entry	Substrate	1a (mol%)	TBHP ^a (mL)	Product(s)	Time(h)	Yield(%) ^b
1		1.0	0.9	C ₆ H ₅ CO ₂ H	8.0	88
2		0.7	0.9	C ₆ H ₅ CO ₂ H	7.5	85
3		0.6	1.0	C ₆ H ₅ CO ₂ H	6.0	92
4		0.6	0.8	C ₆ H ₅ CO	6.5	90
5		0.8	1.0	C ₆ H ₅ CO ₂ H	7.0	82
6		1.0	1.2	C ₆ H ₅ CO ₂ H	8.5	78
7		0.7	0.9		7.0	80
8		0.7	0.9		7.0	78
9		1.0	1.2		10	65
10		1.0	1.2	C ₆ H ₅ CO ₂ H +	8.0	80, 72
11		1.0	1.2	C ₆ H ₅ CO ₂ H +	8.5	75, 70
12		1.0	1.2	C ₆ H ₅ CO ₂ H +	9.0	78, 72
13		1.0	1.2	C ₆ H ₅ CO ₂ H +	8.5	76, 68
14		0.6	1.0	HO ₂ C—(CH ₂) ₄ —CO ₂ H	6.0	86
15		0.6	1.0	HO ₂ C—(CH ₂) ₆ —CO ₂ H	6.0	82
16		0.6	1.0		6.5	75

^a TBHP 5.0-6.0 M solution in decane was used. ^b Yields refer to those of purified products characterized by IR, ¹H, ¹³C NMR spectroscopic data.

(5–20%), were also identified as byproducts of these reactions. The reactions with 30% hydrogen peroxide, however, did not show any selectivity. To avoid the formation of 1,2-diols, the reactions were, in general carried out using TBHP in moisture free *n*-decane-acetonitrile mixture.

As shown in Table 5, a number of aromatic as well as aliphatic olefins were selectively cleaved by the present protocol to yield carboxylic acids in high to excellent yields. Thus, styrene gave an 88% yield of benzoic acid (Table 5, entry 1) and *trans*-stilbene (Table 5, entry 3) afforded 2 equiv of benzoic acid within 6 h. However, the α -substituted aromatic alkene, 1-methyl styrene (Table 5 entry 4) produced acetophenone in 90% yield. In a similar manner oxidation of cinnamyl alcohol and *trans* cinamic acid ethyl ester (Table

5, entries 5 and 6) produced benzoic acid in 82% and 78% yield, respectively. Likewise open chain α -olefins like 1-octene and 1-hexene were easily converted into the respective alkanolic acids of one less carbon in nearly 80% yield (Table 5, entries 7 and 8).

Aromatic rings having localized double bond character as in phenanthrene were also cleaved cleanly under the reaction protocol affording biphenyl dicarboxylic acid (Table 5, entry 9) in 65% yield. It may be noted here that oxidation of phenanthrene to corresponding dicarboxylic acid is usually sluggish.^{16f} The catalyst is found to be equally effective also for the oxidation of aromatic alkene with less double bond character. Thus α,β -unsaturated chalcones (Table 5, entries 10–13) produced carboxylic acids in high yields. Cyclic olefins like cyclohexene, cyclooctene, and 1-methyl cyclo-

Table 6. Oxidation of Alkynes by TBHP Catalyzed by **1a**

Entry	Substrate	1a (mol%)	TBHP ^a (mL)	Product(s)	Time(h)	Yield(%) ^b
1		0.6	1.0	C ₆ H ₅ CO ₂ H	10	85
2		0.6	1.0	C ₆ H ₅ CO ₂ H	10	78
3		0.7	1.0		9.0	80
4		0.8	1.0		9.0	76
5		0.8	1.2		12	70

^a TBHP 5.0–6.0 M solution in decane was used. ^b Yields refer to those of purified products characterized by IR, ¹H, ¹³C NMR spectroscopic data.

Table 7. Oxidation of Aldehyde by TBHP Catalyzed by **1a**

Entry	Substrate	1a (mol%)	TBHP ^a (mL)	Product(s)	Time(h)	Yield(%) ^b
1	C ₆ H ₅ CHO	0.5	0.5	C ₆ H ₅ CO ₂ H	3.5	95
2		0.8	0.7		4.5	80
3		0.7	0.6		4.0	80
4		0.8	0.6		5.0	78

^a TBHP 5.0–6.0 M solution in decane was used. ^b Yields refer to those of purified products characterized by IR, ¹H, ¹³C NMR spectroscopic data.

hexene also were cleaved affording an 86% yield of adipic acid, an 82% yield of suberic acid and an 75% yield of 6-oxoheptanoic acids (Table 5, entries 14–16) respectively.

To exclude the possibility that the complex **1a** just serves as a source of OsO₄ via the oxidative removal of the diamide ligands, two following control experiments were planned. First, a catalytic quantity of OsO₄ was used in place of **1a** for the oxidation of styrene under analogous reaction conditions as described above. The reaction is unclean and produced a mixture of products. Working up of the mixture yielded benzyl alcohol as the major product along with minor quantities of styrene-1,2-diol and benzoic acid. It also contained small quantities of several unidentified products, which could not be separated from the crude mixture. Second, to ascertain the fate of the catalyst after the reaction we have analyzed the ESI-MS spectrum of the reaction mixture that contained a catalytic quantity of **1a**, styrene, and *t*-butylhydroperoxide. A small portion of the mixture after 7 h stirring was evaporated under vacuum, and the residue separated by washing with diethyl ether displayed a peak at *m/z*, 677 amu in acetonitrile. Its simulation matched with a molecular adducts ion [**1a**.styrene]⁺ (Supporting Information, Figure S6) confirming that the catalyst remained intact during the reaction. However, after a very prolonged reaction time (>24 h) the ESI-MS spectrum could not locate the existence of the catalyst indicating that the catalyst decomposes in TBHP. This is not unexpected since cyclic voltammetry of **1a** also showed only an irreversible anodic wave. To confirm it further ESI-MS of a freshly prepared mixture of the catalyst and TBHP in the absence of styrene

was analyzed. ESI-MS of the later mixture indicated rapid decomposition of the catalyst. In another experiment it was possible to show that the complex catalyst is stable in styrene. Thus the results of the above experiments confirm that **1a** acts as a catalyst in bringing about oxidative C–C bond cleavage of olefins by TBHP.

Catalytic activities of the osmium compound **1a** toward the cleavage aromatic and aliphatic alkynes were also studied. Five alkyne substrates were subjected to oxidation, and the results are summarized in Table 6. Both aromatic and aliphatic alkynes produced the corresponding carboxylic acids in high yields (70–85%). Similarly oxidation of aldehydes was also achieved in high yields (Table 7). Control experiments were also performed whereby two aldehydes, namely, benzaldehyde and *n*-octanal, were reacted separately with *t*-butylhydroperoxide without addition of the osmium catalyst. In these cases only partial oxidation of the aldehydes to the corresponding carboxylic acids was observed. In comparison, high yield oxidations (>80%) of the above aldehydes were achieved in the presence of **1a** within 4 h. Similar observation was also noted by others.³³

Conclusion

In this work, we have introduced a one pot synthesis of a family of monooxo osmium(VI) complex (**1**) of *N*-aryl diamide ligand that catalyzes oxidative cleavage of unsatur-

(33) (a) Mannam, S.; Sekar, G. *Tetrahedron Lett.* **2008**, *49*, 1083. (b) Wójtcowicz, H.; Brzyszczyk, M.; Kloc, K.; Młochowski, J. *Tetrahedron* **2001**, *57*, 9743.

ated hydrocarbons with remarkable efficiency. The synthetic methodology involved OsO₄ promoted selective *ortho*-C-N fusion of aromatic amines. This result is in sharp contrast to the available literature of such oxidation reactions and has opened up further the scope of studying aromatic amine fusion reactions using high valent metal oxides as templates. For example, it will be of interest to perform the oxidation reactions of OsO₄ in neat aromatic amines. Our work in this area is continuing. The new osmium complexes have been characterized structurally as well as spectroscopically. Spectral transitions are guided by theoretical studies (DFT). The complex **1a** catalyzes oxidative cleavage of C–C bonds of a variety of alkenes and alkynes by *tert*-butylhydroperoxide in acetonitrile resulting in the formation of the corresponding carboxylic acids or ketones at room temperature. The catalytic potential of the osmium complex for the oxidative bond cleavage of unsaturated hydrocarbons is demonstrated.

Experimental Section

Instrumentation. UV–vis absorption spectra were recorded on a Perkin-Elmer Lambda 950 UV/vis spectrophotometer. ¹H and ¹³C NMR spectra were taken on a Bruker Advance DPX 300 spectrometer. Infrared spectra were obtained using a Perkin-Elmer 783 spectrophotometer. Cyclic voltammetry was carried out in 0.1 M [Bu₄N]ClO₄ solutions using a three-electrode configuration (glassy carbon working electrode, Pt counter electrode, Ag/AgCl reference) and a PC-controlled PAR model 273A electrochemistry system. The *E*_{1/2} for the ferrocenium-ferrocene couple under our experimental condition was 0.39 V. A Perkin-Elmer 240C elemental analyzer was used to collect microanalytical data (C, H, N). ESI mass spectra were recorded on a micro mass Q-TOF mass spectrometer (serial no. YA 263). EPR spectra in the X-band were recorded with a Bruker System EMX spectrometer. A two-electrode capillary served to generate intermediates for the X-band EPR studies.

Materials. The high valent metal oxide OsO₄ was an Aldrich reagent and the solvents used were obtained from Qualigens and MERCK (India). *N*-phenyl-1,2-phenelenediamine was purchased from Aldrich. Tetrabutylammonium perchlorate (TEAP) was prepared and recrystallized as reported earlier.³⁴ All other chemicals were of reagent grade and used as received. **Caution!** OsO₄ and perchlorate salts have to be handled with care and with appropriate safety precautions.

Synthesis. Syntheses of the complexes were carried out by the reaction of osmium(VIII) oxide with the corresponding anilines in refluxing heptane. The complexes **1** (general formula OsOL₂) were obtained as the major products along with some unidentified minor products which are not considered here.

Syntheses of OsOL₂. OsO(L^a)₂ (**1a**): A mixture of 1 g (3.94 mmol) of OsO₄, and 1.49 g (16 mmol) of aniline in heptane was refluxed for 4 h in dry N₂ atmosphere. During this period the color of the solution changed from red to dark brown. The crude mass thus obtained by evaporation of the solvent was dissolved in a minimum volume of dichloromethane and loaded on a preparative alumina TLC plate for purification. Toluene was used as the eluent. A broad reddish brown zone was collected, and the solvent was

evaporated under vacuum. The residue was crystallized by slow evaporation of a dichloromethane-hexane solution mixture. Yield: 42%. IR (KBr, cm⁻¹): 3450 [ν (N–H)], 890 [ν (Os=O)]. ESI-MS, *m/z*: 572 [MH]⁺. Anal. Calcd for C₂₄H₂₀N₄O₅: C, 50.46; H, 3.52; N, 9.79 Found: C, 50.51; H, 3.53; N, 9.81.

The substituted complexes **1b** and **1c** were synthesized similarly using the appropriate *para*-substituted anilines in place of aniline. Their yields and characterization data are as follows. OsO(L^b)₂ (**1b**). Yield: 35%. IR (KBr, cm⁻¹): 3400 [ν (N–H)], 890 [ν (Os=O)]. ESI-MS, *m/z*: 628 [MH]⁺. Anal. Calcd for C₂₈H₂₈N₄O₅: C, 53.61; H, 4.49; N, 8.90. Found: C, 53.65; H, 4.50; N, 8.91. OsO(L^c)₂ (**1c**). Yield: 40%. IR (KBr, cm⁻¹): 3400 [ν (N–H)], 890 [ν (Os=O)]. ESI-MS, *m/z*: 709 [MH]⁺. Anal. Calcd for C₂₄H₁₆Cl₄N₄O₅: C, 40.65; H, 2.25; N, 7.86 Found: C, 40.67; H, 2.27; N, 7.90.

Reaction of OsO₄ with Preformed HL^a. To a solution of 0.25 g (1.1 mmol) of *N*-phenyl-1,2-phenelenediamine (HL^a) in 30 mL of heptane was added 0.1 g (0.39 mmol) of osmium tetroxide under dry N₂ atmosphere. The resulting mixture was refluxed for 4 h after which the solution was dried under reduced pressure. The crude mass, thus obtained, was loaded on a preparative alumina TLC plate for purification using toluene as the eluent. A red band of 5-phenyl-3-phenylimino-3,5-dihydro-phenazine-2-ylamine (phenz), which moved just ahead of the broad reddish brown band, was collected. It was evaporated to dryness and crystallized from CH₂Cl₂–C₆H₁₄ solvent mixture. The characterization data are as follows:

Yield: 16%, ESI-MS, *m/z*: 363 [phenzH]⁺. Anal. Calcd for C₂₄H₁₈N₄: C, 79.51; H, 4.98; N, 15.42 Found: C, 79.53; H, 5.01; N, 15.46.

The second broad brown band was also collected from the TLC plate. Subsequent evaporation of the solution followed by crystallization by slow diffusion of hexane into the solution of the compound in dichloromethane yielded a crystalline brown compound, which is identical in all respects to the structurally characterized sample, **1a**. The yield of **1a** from the above reaction was 94%.

Olefin Oxidation. Olefin oxidation reactions were performed by using a common procedure. A representative example (oxidation of stilbene) is elaborated below. However, the duration of the reaction time varied for different substrates as noted in Tables 5 and 6.

To a dry acetonitrile (1.5 mL) solution of stilbene (0.180 g, 1 mmol) was added *tert*-butylhydroperoxide in decane (1.0 mL) at room temperature followed by the addition of (0.6 mol %) of the catalyst **1a**. The reaction mixture was allowed to stir for 6.0 h. The reaction mixture was then extracted with ethyl acetate, washed with brine, and dried over Na₂SO₄. Evaporation of the solvent under reduced pressure left the crude product. After column chromatography 0.224 g (92%) of pure benzoic acid was isolated. The melting point and spectroscopic data (IR, ¹H and ¹³C NMR) of the products were in good agreement with those of an authentic sample of benzoic acid.

The above procedure was also followed for the oxidations of alkynes and aldehydes.

Crystallography. Crystallographic data of the compound **1a** are collected in Table 8. Suitable X-ray quality crystals of **1a** were obtained by slow evaporation of a dichloromethane-hexane solution of the compound. All data were collected on a Bruker SMART APEX diffractometer, equipped with graphite monochromated Mo K α radiation ($\lambda = 0.71073$ Å) and were corrected for Lorentz-polarization effects. A total of 6343 reflections were collected, out of which 2514 were unique (*R*_{int} = 0.0401), satisfying the (*I* > 2 σ (*I*)) criterion, and were used in subsequent analysis.

(34) Goswami, S.; Mukherjee, R. N.; Chakravarty, A. *Inorg. Chem.* **1983**, *22*, 2825.

(35) (a) Sheldrick, G. M. *Acta Crystallogr., Sect. A* **1990**, *46*, 467. (b) Sheldrick, G. M., *SHELXL 97. Program for the refinement of crystal structures*; University of Göttingen; Göttingen, Germany, 1997.

Table 8. Crystallographic Data of **1a**

	1a
empirical formula	C ₂₄ H ₂₀ N ₄ OsO
molecular mass	570.68
temperature (K)	293(2)
crystal system	monoclinic
space group	<i>P2₁/n</i>
<i>a</i> (Å)	14.036(2)
<i>b</i> (Å)	4.9270(9)
<i>c</i> (Å)	14.698(3)
α (deg)	90
β (deg)	95.070(3)
γ (deg)	90
<i>V</i> (Å ³)	1012.5(3)
<i>Z</i>	2
<i>D</i> _{calcd} (g/cm ³)	1.872
cryst. dimens. (mm)	0.12 × 0.16 × 0.32
θ range for data coll (deg)	2.8–28.4
GOF	1.144
reflns. collected	6343
unique reflns.	2514
largest diff. between peak and hole (e Å ⁻³)	1.44, –1.35
final <i>R</i> indices [<i>I</i> > 2 σ (<i>I</i>)]	<i>R</i> 1 = 0.0393 w <i>R</i> 2 = 0.0893

The structure was solved by employing the SHELXS-97 program package^{35a} and refined by full-matrix least-squares based on *F*² (SHELXL-97).^{35b} During refinement, the N-phenyl 1,2-phenylene diamide ligand was found to be disordered (Supporting Information, Figure S5) over two orientations (N1, C1, C2, C3, C4, C5, C6, C7, C8, C9, C10, C11, C12 and N1', C1', C2', C3', C4', C5', C6', C7', C8', C9', C10', C11', C12') with 0.5:0.5 occupancy ratio. The final refinement was done with SHELX restraints SIMU for disordered ligands and ISOR for N1, N1' and N2. The final difference Fourier map does not show any chemically significant peak. All hydrogen atoms were added in calculated positions. All aromatic rings were fitted and refined as regular hexagon.

Computational Details. Density functional theory (DFT) calculations were performed for the C₂ symmetric Os(VI) oxo-compound **1a** and its reduced anionic form [**1a**][−]. The calculations utilized a combination of the hybrid PBE1PBE exchange-correlation functional³⁶ with Ahlrichs' triple- ζ valence basis sets augmented by one set of polarization functions (def-TZVP); for osmium, the

corresponding effective core potential (ECP) basis set of similar valence quality was used.³⁷ Electronic excitation energies of **1a** were calculated using time-dependent density functional formalism (TDDFT) utilizing the same functional-basis set combination which was used in the geometry optimization. All calculations were performed with the Turbomole 5.9.1 program package.³⁸

Acknowledgment. Financial support from the Department of Science and Technology (DST)(Project SR/S1/IC-24/2006) New Delhi, is gratefully acknowledged. S.S. thanks the Council of Scientific and Industrial Research, New Delhi for his fellowship. Crystallography was performed at the DST-funded National Single Crystal Diffractometer Facility at the Department of Inorganic Chemistry, IACS. Thanks are due to Professor Wolfgang Kaim and Dr. Biprajit Sarkar for EPR measurements. H.M.T. thanks the Academy of Finland and the University of Jyväskylä for their generous financial support. We are thankful to the reviewers for their constructive suggestion at the revision stage.

Supporting Information Available: X-ray crystallographic files in CIF format for **1a**; figures of ¹H NMR spectra of **1a** (S1); ¹³C NMR spectra of **1b** (S2), Hammett's plot (S3), selected orbital isosurfaces of **1a** (S4), ORTEP and atom numbering scheme of **1a** (S5) are provided and ESI-MS spectrum of [**1a**.styrene]⁺ (S6). This material is available free of charge via the Internet at <http://pubs.acs.org>.

IC801352D

- (36) (a) Perdew, J. P.; Burke, K.; Ernzerhof, M. *Phys. Rev. Lett.* **1996**, *77*, 3865. (b) Perdew, J. P.; Burke, K.; Ernzerhof, M. *Phys. Rev. Lett.* **1997**, *78*, 1396. (c) Perdew, J. P.; Ernzerhof, M.; Burke, K. *J. Chem. Phys.* **1996**, *105*, 9982. (d) Ernzerhof, M.; Scuseria, G. E. *J. Chem. Phys.* **1999**, *110*, 5029.
- (37) (a) Schaefer, A.; Horn, H.; Ahlrichs, R. *J. Chem. Phys.* **1992**, *97*, 2571. (b) Schaefer, A.; Huber, C.; Ahlrichs, R. *J. Chem. Phys.* **1994**, *100*, 5829.
- (38) *TURBOMOLE, Program Package for ab initio Electronic Structure Calculations*, Version 5.9.1; University of Karlsruhe: Karlsruhe, Germany, 2007. (b) Ahlrichs, R.; Bär, M.; Häser, M.; Horn, H.; Kölmel, C. *Chem. Phys. Lett.* **1989**, *162*, 165.